Investigation of the distribution of laser damage precursors at 1064 nm, 12 ns on Niobia-Silica and Zirconia-Silica mixtures

Xinghai Fu, Andrius Melnikaitis, Laurent Gallais, Simonas Kicas, Ramutis Drazdys, Valdas Sirutkaitis, Mireille Commandre

Investigation of the distribution of laser damage precursors at 1064 nm, 12 ns on Niobia-Silica and Zirconia-Silica mixtures

X. Fu,[1] A. Melnikaitis,[2] L. Gallais, [1,*] S. Kiáčas,[3] R. Drazdys,[3]V. Sirutkaitis,[2] and M. Commandré[1]

[1]*Institut Fresnel, CNRS, Université d'Aix-Marseille, Ecole Centrale Marseille, Campus de St Jérôme, 13013 Marseille, France*
[2]*Laser Research Center, Vilnius University, Saulėtekio al. 10, 10223 Vilnius, Lithuania*
[3]*State Research Institute for Physical Sciences and Technology, Savanoriu, pr. 231, 02300 Vilnius, Lithuania*
[*]*laurent.gallais@fresnel.fr*

Abstract: Simple Nb_2O_5, ZrO_2, SiO_2 oxide coatings and their mixtures with SiO_2 have been prepared by the Ion Beam Sputtering (IBS) technique. The Laser-Induced Damage of these samples has been studied at 1064 nm, 12 ns. The laser induced damage threshold (LIDT) decreases in both sets of the mixtures with the volumetric fraction of high index material. We find that the nanosecond LIDT of the mixtures is related to the band gap of the material as it has been widely observed in the subpicosecond regime. The laser damage probability curves have been fitted firstly by a statistical approach, i.e. direct calculation of damage precursor density from damage probability and secondly by a thermal model based on absorption of initiator. The distributions of damage precursors versus fluence extracted from these fittings show a good agreement. The thermal model makes it possible to connect damage probability to precursor physical properties. A metallic defect with a maximum radius of 18 nm was proposed to the interpretation. The critical temperature in the laser damage process exhibited a dependence on the band-gap of the material.

OCIS codes: (310.0310) Thin films; (140.3330) Laser damage.

References and links

1. H. A. Macleod, *Thin-Film Optical Filters*, 4th ed. (CRC Press, USA, 2010).
2. S. Chao, W. H. Wang, and C. C. Lee, "Low-loss dielectric mirror with ion-beam-sputtered TiO2-SiO2 mixed films," Appl. Opt. **40**(13), 2177–2182 (2001).
3. B. J. Pond, J. I. Debar, C. K. Carniglia, and T. Raj, "Stress reduction in ion beam sputtered mixed oxide films," Appl. Opt. **28**(14), 2800–2805 (1989).
4. S. Papernov and A. W. Schmid, "Correlations between embedded single gold nanoparticles in SiO2 thin film and nanoscale crater formation induced by pulsed-laser irradiation," J. Appl. Phys. **92**(10), 5720–5728 (2002).
5. M. D. Feit, A. M. Rubenchik, and M. Runkel, "Analysis of bulk DKDP damage distribution, obscuration, and pulse-length dependence," Proc. SPIE **4347**, 383–388 (2001).
6. M. Alvisi, M. Di Giulio, S. G. Marrone, M. R. Perrone, M. L. Protopapa, A. Valentini, and L. Vasanelli, "HfO2 films with high laser damage threshold," Thin Solid Films **358**(1-2), 250–258 (2000).
7. D. W. Zhang, Y. S. Huang, Z. J. Ni, S. L. Zhuang, J. D. Shao, and Z. X. Fan, "Preparation of high laser induced damage threshold antireflection film using interrupted ion assisted deposition," Opt. Express **15**(17), 10753–10760 (2007).
8. T. A. Laurence, J. D. Bude, S. Ly, N. Shen, and M. D. Feit, "Extracting the distribution of laser damage precursors on fused silica surfaces for 351 nm, 3 ns laser pulses at high fluences (20-150 J/cm$^{2)}$," Opt. Express **20**(10), 11561–11573 (2012).
9. D. Nguyen, L. A. Emmert, I. V. Cravetchi, M. Mero, W. Rudolph, M. Jupe, M. Lappschies, K. Starke, and D. Ristau, "$Ti_xSi_{1-x}O2$ optical coatings with tunable index and their response to intense subpicosecond laser pulse irradiation," Appl. Phys. Lett. **93**(26), 261903 (2008).
10. M. Jupé, L. Jensen, A. Melninkaitis, V. Sirutkaitis, and D. Ristau, "Calculations and experimental demonstration of multi-photon absorption governing fs laser-induced damage in titania," Opt. Express **17**(15), 12269–12278 (2009).
11. A. Melninkaitis, T. Tolenis, L. Mažulė, J. Mirauskas, V. Sirutkaitis, B. Mangote, X. Fu, M. Zerrad, L. Gallais, M. Commandré, S. Kičas, and R. Drazdys, "Characterization of zirconia- and niobia-silica mixture coatings produced by ion-beam sputtering," Appl. Opt. **50**(9), C188–C196 (2011).
12. M. Mende, L. Jensen, H. Ehlers, W. Riggers, H. Blaschke, and D. Ristau, "Laser-induced damage of pure and

#173024 - $15.00 USD Received 20 Jul 2012; revised 24 Aug 2012; accepted 28 Aug 2012; published 2 Nov 2012

mixture material high reflectors for 355nm and 1064nm wavelength," Proc. SPIE **8168**, 816821, 816821-11 (2011).
13. J. Capoulade, L. Gallais, J.-Y. Natoli, and M. Commandré, "Multiscale analysis of the laser-induced damage threshold in optical coatings," Appl. Opt. **47**(29), 5272–5280 (2008).
14. L. Lamaignère, S. Bouillet, R. Courchinoux, T. Donval, M. Josse, J. C. Poncetta, and H. Bercegol, "An accurate, repeatable, and well characterized measurement of laser damage density of optical materials," Rev. Sci. Instrum. **78**(10), 103105 (2007).
15. L. Jensen, S. Schrameyer, M. Jupé, H. Blaschke, and D. Ristau, "Spotsize dependence of the LIDT from the NIR to the UV," Proc. SPIE **7504**, 75041E, 75041E-8 (2009).
16. M. D. Feit and A. M. Rubenchik, "Implications of nanoabsorber initiators for damage probability curves, pulselength scaling and laser conditioning," Proc. SPIE **5273**, 74–82 (2004).
17. L. Gallais, J. Capoulade, J. Y. Natoli, and M. Commandré, "Investigation of nanodefect properties in optical coatings by coupling measured and simulated laser damage statistics," J. Appl. Phys. **104**(5), 053120 (2008).
18. R. H. Picard, D. Milam, and R. A. Bradbury, "Statistical analysis of defect-caused laser damage in thin films," Appl. Opt. **16**(6), 1563–1571 (1977).
19. J. O. Porteus and S. C. Seitel, "Absolute onset of optical surface damage using distributed defect ensembles," Appl. Opt. **23**(21), 3796–3805 (1984).
20. J. H. Weaver, D. W. Lynch, and C. G. Olson, "Optical properties of niobium from 0.1 to 36.4 eV," Phys. Rev. B **7**(10), 4311–4318 (1973).
21. D. R. Lide, *Handbook of Chemistry and Physics*, 87th ed. (CRC press, USA 2007).
22. C. W. Carr, H. B. Radousky, A. M. Rubenchik, M. D. Feit, and S. G. Demos, "Localized dynamics during laser-induced damage in optical materials," Phys. Rev. Lett. **92**(8), 087401 (2004).

1. Introduction

For optical interference coatings design requirements, the mixing of two simple materials have the competence to offer tailored refractive index covering the range between the two materials [1]. The employment of the mixed coatings avoids the discrete layer interfaces and some improvements compared to classical designs have been observed in optical properties such as reduction of the optical losses [2] and residual stress [3]. The high power laser application necessitates the research on the laser irradiation resistance of optical coatings. Efforts are dedicated into the understanding of laser damage effects [4, 5] and the improvement of the laser induced damage threshold (LIDT) [6, 7] by the studying the pure materials in nano and femto second regime. In femtosecond regime the LIDT shows strong band gap dependence. In nanosecond regime, it is well known that laser damage is related to precursors and many studies are devoted to the analysis of density of precursors versus fluence [8]. Few studies are in the subject of mixed coating. The studies of mixed coating carried out in the pico and femtosecond regime [9–11] confirm the band gap dependence of the LIDT values. In nanosecond regime, the LIDT of high reflectors based on multiple layers mixed coating is obtained while no comments relates to the precursors neither to the band gap of the material [12].

In the paper the mixtures of ZrO_2/SiO_2 and Nb_2O_5/SiO_2 previously characterized in femtosecond regime are studied now in the nanosecond regime in order to establish a relation between the damage threshold and the composition of the mixtures as well as their physical properties especially the band gap. A special interest will be presented in the precursor densities versus fluence. For these purposes LIDT performances of the two sets of mixtures with different compositions were characterized in the nanosecond regime at 1064nm by using a tightly focused laser beam. The laser damage is linked to absorbing defects in the nanosecond regime therefore the damage initiation is localized and probabilistic. For the analysis of distribution of laser damage precursor density, we applied two models, the statistical approach based on a power law distribution of precursors versus fluence, and a thermal model concerning the defect size, complex index and density, critical temperature, thermal conductivity, etc. The distributions of laser damage precursor density from the two models are compared. From the thermal model we extract the critical temperatures by fitting the experimental data and the discussion is made on the relation between the critical temperatures and the band gap of material.

2. Experimental details

2.1. Samples fabrication and properties

Single layer films of simple Nb_2O_5, ZrO_2, SiO_2 oxide and their mixtures Nb_2O_5/SiO_2, ZrO_2/SiO_2 were prepared using a modified IBS technique on 1mm thick fused-silica (UV grade KU1 glass) substrates from the same polishing batch. Among the mixtures, the SiO_2 fraction was varied from approx. 25 to 75% with a step of 25%. We name these samples

#173024 - $15.00 USD Received 20 Jul 2012; revised 24 Aug 2012; accepted 28 Aug 2012; published 2 Nov 2012

"low-silica", "half-silica" and "high-silica" respectively. A detailed description can be found in Ref [11], the growth conditions of the samples, the LIDT measurement in femtosecond regime as well as the presentations of the non-destructive characterization techniques (Atomic Force Microscopy, Angle-Resolved Scattering, Total Integrated Scattering, X-Ray Diffraction). We have summarized the properties of interest for this paper in the left part of Table 1. The volumetric fractions of the high index materials are estimated by spectrophotometric measurement and effective medium approximation (EMA). The band gap values were determined from absorption spectra by using three different approaches: linear fitting of so-called Tauc (E_{gT}) and Cody (E_{gC}) plots as well as the inflection point method derived from the Urbach equation (E_{gU}), the related precision is about 3% for a given method. The definition of the band gap plays a role of importance in the absolute values. The band gaps based on the Tauc and Cody plots were similar while the last approach resulted in larger values. Whatever the approach the band gap evolution versus the film composition is the same, we observe an increase of the band gap versus the SiO_2 fraction of the mixture. The stoichiometry deviation (present in the right part of Table 1) has been determined by Rutherford Backscattering Spectroscopy (RBS) with an incident beam diameter of 1.5 mm, the standard error of estimated values does not exceed 2.5%. The results show that most of the films are sub-stoichiometric, except the simple SiO_2, simple Nb_2O_5 and high-silica mixture with ZrO_2. The stoichiometry deviations are 2% and 6% respectively for Nb_2O_5 and ZrO_2 films. For mixtures, the deviations increase with the fraction of high index materials.

2.2. Laser damage probability measurements at 1064 nm, 12 ns

In this paper the LIDT in nanosecond regime was studied with a Nd: YAG laser operating in the single longitudinal mode regime (Quantel YG980, wavelength 1064nm, repetition rate 10 Hz, effective pulse duration 12ns). The laser beam was focused into a spot with a diameter of 25.4 µm (taken at $1/e^2$) at the sample surface at the normal incidence, and the coated side facing the incoming beam. A small beam diameter has been chosen to be as close as possible to intrinsic damage conditions. The damage detection was based on an image acquisition system and algorithm that compares the images before and after irradiation. A detailed presentation of the experimental set-up and the automatic procedure can be found in Ref [13]. The damage probability was obtained with a 1 on 1 mode. The probability curve was plotted with 20 different fluencies and 50 sites were tested at each fluence. LIDT is defined as the maximum fluence with zero damage probability. The damage thresholds that we report are then representative of these test conditions, with an objective of making comparative studies of the intrinsic behavior of the mixtures, it is why we choose a small beam diameter about 25 µm. For applications and when functional LIDT is needed, other kinds of measurement procedure such as the damage thresholds under multiple shots or with the total surface of the sample tested (raster scan procedure [14]) are more appropriated.

Table 1. Summary of the properties of interest of the films

Sample	SiO2 volumetric fraction (%)	n_{1064}	Thick -ness (nm)	Band gap (eV) E_{gT}/E_{gU}	LIDT at 530fs, 1030nm (J/cm^2)	LIDT at 12ns, 1064nm (J/cm^2)	Stoichiometry deviation(%) (± 2.5%)
		Simple Oxides				Simple Oxides	
SiO_2	-	1.48	1090	7.5/-	6.0	300.6	0
Nb_2O_5	-	2.23	717	3.46/3.92	1.1	10.9	–2
ZrO_2	-	2.09	759	4.74/5.29	2.4	27.5	–6
		Mixed Nb_2O_5/ SiO_2				Mixed Nb_2O_5/ SiO_2	
High-silica	66.4	1.71	939	3.94/4.80	3.0	81.0	–6
Half-silica	39.6	1.92	838	3.74/4.37	2.0	28.2	–7
Low-silica	20.6	2.07	773	3.61/4.18	1.5	19.3	–11
		Mixed ZrO_2/ SiO_2				Mixed ZrO_2/ SiO_2	
High-silica	70.8	1.66	970	5.38/-	4.5	77.6	+ 1
Half-silica	47.7	1.81	885	5.18/5.99	3.6	45.7	–1
Low-silica	24.8	1.96	811	4.94/5.61	2.9	35.9	–15

#173024 - $15.00 USD Received 20 Jul 2012; revised 24 Aug 2012; accepted 28 Aug 2012; published 2 Nov 2012

3. Results

3.1 Damage thresholds

The results of LIDT (1064 nm, 12 ns) are given in the Table 1 at right. In Fig. 1(a) the LIDT evolution for two sets of samples (ZrO_2 and Nb_2O_5) is plotted versus the volumetric fraction of the high index material. We note that the simple SiO_2 film has the best performance in the damage resistance measurement. We observe that the increase concentration in the mixture of the high refractive index materials ZrO_2 or Nb_2O_5 results in continuously decreasing damage threshold. The LIDT of simple SiO2 is as high as 300 J/cm^2 while the LIDT of simple Nb_2O_5 is found 11 J/cm^2. The reported high LIDT value of simple SiO_2 is related to the spotsize dependence [15] for laser beam size smaller than 100 µm. The simple oxide ZrO_2 has a better damage resistance than the simple Nb_2O_5. This is still true for the associated mixtures. For the sake of comparison we plot on the same figure the LIDT evolution in the femtosecond regime [11] which shows a similar behavior. In Fig. 1(b) we have plotted LIDT values versus band gap determined by the linear fitting of Tauc plot. The LIDT is clearly related to the band gap in the nanosecond regime as it has been observed for subpicosecond pulses. This can seem surprising if we consider that the nanosecond damage is initiated by defects. Firstly it is well known that the presence of defects in an insulating material can be associated to electronic levels in the forbidden band which can modify the band gap. In the case of oxides mixture, the nanosecond damage precursors could have this kind of behavior. Secondly our measurements were performed for small beam and in this case the LIDT values are close to the intrinsic ones.

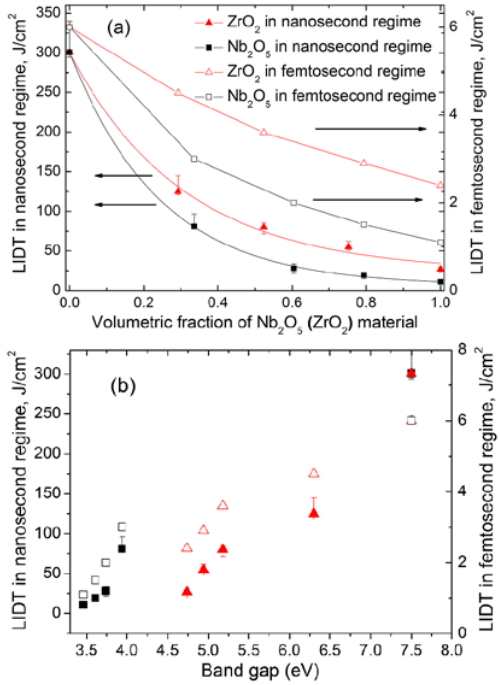

Fig. 1. Damage thresholds of Nb_2O_5/SiO_2 and ZrO_2 Nb_2O_5/SiO_2 mixtures. (a) Damage thresholds versus the volumetric fraction of high index material obtained at 1064nm, 12 ns, 1 on 1 mode (left scale, solid symbols). For the sake of comparison we plot the damage thresholds mentioned in Ref [11]. at 530 fs, 1030nm (right scale, open symbols), the solid curves are drawn to show their evolution tendencies. (b) Damage thresholds versus the band gap of the material with the same symbols.

3.2 Laser damage probability curves

The evolution of the probability curves with the mixture composition is shown in Fig. 2. The experimental data are plotted with error bars. Both sets of the curves reveal that the sample of higher SiO_2 composition is more stable and has a smaller probability to initiate

#173024 - $15.00 USD Received 20 Jul 2012; revised 24 Aug 2012; accepted 28 Aug 2012; published 2 Nov 2012

damage. Thus in those having higher SiO_2 fraction, a higher fluence is required to attain 100% probability, for example, 60 J/cm^2 for simple Nb_2O_5 film, 130 J/cm^2 for low-silica mixture and 170 J/cm^2 for half-silica mixture. The experimental data are fitted thanks to two models, firstly a statistical approach, i.e. direct calculation of damage precursor densities from damage probabilities [8, 14], and secondly a thermal model based on absorption of initiators [16, 17]. We will detail these models and the fitting method used in the paper in the following section IV. The fitting results and especially the distributions of defect densities versus fluence are discussed in section IV.

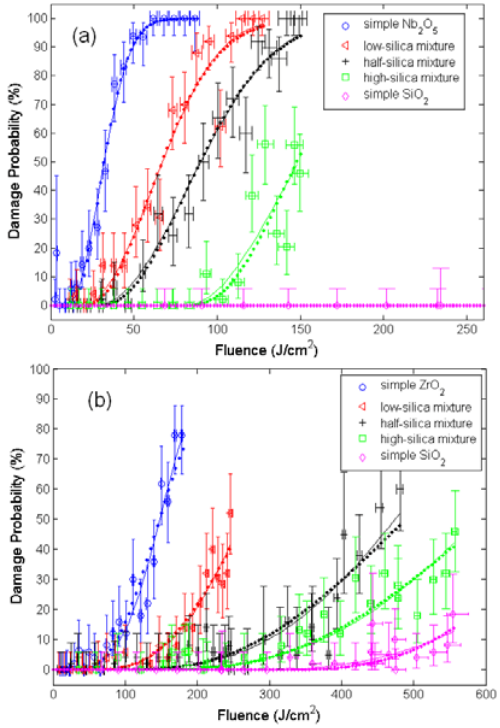

Fig. 2. LIDT Performances of two sets of mixtures: (a) Nb_2O_5/SiO_2 (b) ZrO_2/SiO_2. The probability curves are fitted by the statistical approach (dot line) and the thermal model (solid line).

3.3 Damage morphologies

The morphologies of damage areas were obtained by a Nomarski microscope. Some typical images are presented in Fig. 3.

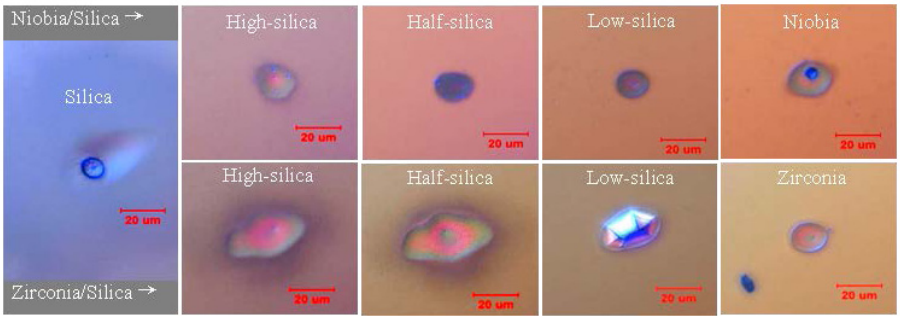

Fig. 3. The morphology of damages in single layer coatings induced by nanosecond laser pulses with a diameter of 25.4 µm at 1/e^2: (top) Nb_2O_5/SiO_2 (bottom) ZrO_2/SiO_2.

#173024 - $15.00 USD Received 20 Jul 2012; revised 24 Aug 2012; accepted 28 Aug 2012; published 2 Nov 2012

As a small laser beam was used, we note that all the damage spots consist of a burned region with one melted dot in the center, this fact ensures the feasibility of evaluation of the damage precursor density from damage probability. In the case of Nb_2O_5 and its mixtures, with the reduction of the silica fraction, the irradiated region becomes rough and the melted dot become remarkable. For the samples of ZrO_2 and its mixtures, we observe delamination effects in the damage zone and a crater in the simple ZrO_2 film.

4. Discussion

As it has been mentioned above, up to now there is a lack of LIDT data about the laser damage resistance performance of metal oxide mixtures in the nanosecond regime and its appropriate comparison to classical oxide materials. In this section analysis of obtained data is performed.

The process of IBS co-deposition of oxides from two metallic targets under a reactive partial pressure can lead to some defects in the films that act as damage precursors and decrease the LIDT. We firstly present the statistical approach of damage precursor density from the probability curves based on a power law distribution of precursors versus fluence. Then the thermal model is applied to study from a fundamental point of view the influence of defects (size, density and nature), and their environment (optical and thermal properties of the films) on the laser damage resistance. The damage precursor densities are obtained and the comparison is conducted.

4.1. Models

4.1.1 Statistical approach model

The damage probability adheres to a Poisson distribution [18] and has a dependency to the damage precursor density *D(F)*,

$$P(F,S) = 1 - \exp(-D(F) \cdot S) \tag{1}$$

where *D(F)* is the number of defects per unit of surface and *S* is the surface of the region where the fluence is greater than the threshold fluence F_{th}.

With an assumption that no precursor exists at the fluence below the threshold F_{th}, this damage precursor density *D(F)* could be estimated for higher fluences by a power law [19],

$$D(F) = \alpha (F - F_{th})^{\beta} \tag{2}$$

Where α, β and F_{th} are fitting parameters.

Given the Gaussian effective area and the damage probability curve from the experiment, α, β and F_{th} are then determined by a least squares fitting. The result will be discussed in terms of precursor density distribution in section D. The main limitation of this approach is the absence of any information on the nature of precursors and the material. However it is interesting to relate these natures to the laser damage phenomena.

4.1.2 Thermal model

Based on the assumption that coatings contain some absorbing defects, we use a model considering initiation of damage by the photo-induced thermal effect. This model is briefly described here in order to identify the parameters of interest, however a detailed description can be found in Ref [16]. and [17].

The potential defects are considered to be either dielectric or metallic particles embedded in the coating, characterized by their complex index $n' + i \cdot n''$. The absorbed power is calculated with the Mie theory as a function of the particle size (an example of such a calculation is given in Fig. 4). The temperature increase of the surrounding medium caused by heat transfer can be estimated with classical heat diffusion calculations [16]. Assuming that the damage occurs while the temperature reaches a critical point *Tc*, we obtain the critical fluence i.e. the fluence that can induce damage as a function of defect size *R* (see for instance Fig. 5). A size distribution of defects is needed and we employed a power law [16]:

$$\rho(R) = A / R^{p} \tag{3}$$

#173024 - $15.00 USD Received 20 Jul 2012; revised 24 Aug 2012; accepted 28 Aug 2012; published 2 Nov 2012

where p and A are fitting parameters. Then $D(F)$ will be given by

$$D(F) = \int_{R\,\min}^{R\,\max} \rho(R)\,dR \tag{4}$$

R_{max} and R_{min} are the boundaries of the integral domain defined in Fig. 5 by the fluences from the laser damage threshold F_{th} to F. The damage probability is calculated in the same way by the Eq. (1). The advantage of this model is to give information on the potential nature and the size of the defect, and to allow a more physical insight of the damage mechanisms.

4.2 Initiating defects

The supplementary tests of the coating atomic structure by using Rutherford Backscattering Spectroscopy, indicates an incomplete oxidation of the mixture films (Table 1). Thus metallic particles (coming from the metallic target) and off-stoichiometric oxide clusters can be considered as reasonable sources of absorption, and therefore damage, in the films. We will then consider these two potential sources and try to estimate with the thermal model if these defects can be responsible for damage, and what should be their size and absorption.

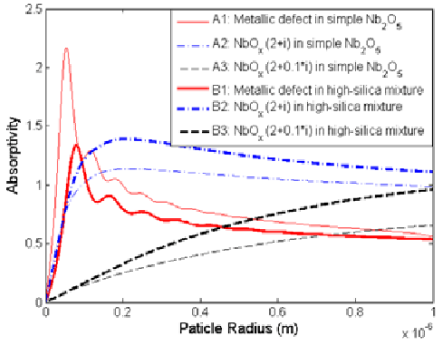

Fig. 4. Absorptivity of defects with different complex index versus defect size. A and B represent the different media simple, Nb_2O_5 (A) and its high-silica mixture (B); the numbers represent the type of defect, metallic defect with n = 1.5 + 5•i (No.1), NbO_x with n = 2 + i (No.2). NbO_x with n = 2 + 0.1•i (No.3).

The damage process is initiated by the absorption of laser energy. As said previously we have considered for this discussion two potential candidates: metallic inclusion with a strong absorbing capacity and off-stoichiometric oxide mixture particles with a weaker absorbing capacity noted as NbO_x or ZrO_x.

By utilizing Mie theory the absorptivity was calculated on the different types of initiators embedded in the coatings. The absorptivity is defined as $a = \sigma/(\pi R^2)$, where σ is the absorption cross section and R the particle radius. For illustration we detail an example of calculation of absorptivity in Fig. 4. The two considered mediums are Nb_2O_5 (A1, A2, A3) drawn with thin lines and its high-silica mixture (B1, B2, B3) plotted with thick lines. The three types of initiator under consideration are the metallic inclusion with complex index of 1.5 + 5·i (A1, B1) which is the value of metallic niobium at 1064 nm [20], and NbO_x inclusions with two complex index of 2 + i (A2, B2) and 2 + 0.1·i (A3, B3), where the different extinction coefficients were chosen to distinguish the different absorbing capacities.

We see that whatever the medium, the absorptivity of a metallic inclusion (curves A1, B1) presents a peak (which can be as high as 2.2 when embedded in Nb_2O_5 and 1.3 in its high-silica mixture) for small particle radius, while the NbO_x with an extinction coefficient of 0.1 has a continuously increasing absorbing capacity with the particle size (curves A3, B3). The NbO_x with an extinction coefficient of 1 presents a high absorbing capacity for the particle radius larger than 100 nm (curves A2, B2). Depending on the metallic or dielectric nature of the defect, we then see clearly that different sizes of defect will be critical. This is illustrated in Fig. 5 where we have plotted the critical fluences versus the

#173024 - $15.00 USD Received 20 Jul 2012; revised 24 Aug 2012; accepted 28 Aug 2012; published 2 Nov 2012

partical radius. The critical fluences duplicate the variation law of the absorptivity curves but in an inverse order. We note that there is a minimum for every curve which corresponds to the most dangerous absorber size. For example, the most dangerous inclusion size is 61 nm for the metallic defect in the simple Nb_2O_5 film corresponding to a critical fluence of 0.07 J/cm^2, 85 nm for the metallic defect in the high-silica mixture with a critical fluence of 0.09 J/cm^2, 121 nm for the NbO_x (2 + i) defect in both films where the critical fluence is 0.1 J/cm^2. For the NbO_x (2 + 0.1*i) defect, these sizes come up to 218 nm and 267 nm owning the critical fluences of 0.62 and 0.5 J/cm^2 respectively. By comparing these values of the critical fluence to the LIDT of our work which varies from 11 to 300 J/cm^2 (see Fig. 1), we can say that the defects are present in the films with sizes smaller than their most dangerous size. Thus we only use the left part of the theses curves in our case. At this level it is not possible to discriminate which between metallic or dielectric precursors can be involved in damage initiation.

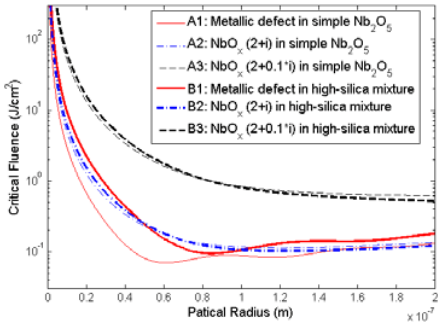

Fig. 5. Critical fluence calculated for metallic and NbO_x defects in simple Nb_2O_5 and its high-silica mixture.

4.3 Fitting method

Many parameters are involved in the calculation of the damage probability thanks to the thermal model. Firstly we have the parameters related to the absorbing defect, real and imaginary parts of the complex index, defect density distribution versus radius (A, p, R_{min}, R_{max}), also mass density and heat capacity. Secondly the parameters related to the matrix film, thermal conductivity and refractive index and thirdly the critical temperature. As most of these parameters remain unknown and could hardly be measured, we make some reasonable simplifications to reduce the fitting parameters. We assume that the defects in the simple materials and their mixtures own the same characteristics (complex index, size distribution) related to the deposition method and conditions. The mass density and heat capacity have a negligible influence in their variation domain, they are fixed at 8570 kg/m^3 and 265 J·kg^{-1}·K^{-1} for the whole set of probability curves. The thermal conductivity is 1.4 W·m^{-1}·K^{-1} for the fused silica at 273 K and 2 W·m^{-1}·K^{-1} for ZrO_2 at 373 K [21], since the values for the thin films tested in this paper are unknown, we keep the thermal conductivity 1.5 W·m^{-1}·K^{-1} for all the samples.

With the assumptions above, we are able to evaluate the critical temperatures of each sample from its LIDT value. Comparing the different critical fluences at the same particle radius in the left part of Fig. 5, we note that only the metallic defect can generate a large difference between the critical fluences, this performance coincides with the experimental results in Fig. 1. Consequently a type of metallic defect with a complex index of 0.3 + 6•i and with its sizes under 18 nm as an example is considered as the laser damage precursor for all the samples, simple oxides and their mixtures. The critical temperatures are obtained based on this kind of precursor.

The probability curves are fitted afterwards with both the thermal method given in the previous paragraph (same kind of defect and maximum size for all the samples) and the statistical approach. The fittings follow the method of least square and the fitting quality is evaluated by a minimized sum of squares, noted as S in following.

#173024 - $15.00 USD Received 20 Jul 2012; revised 24 Aug 2012; accepted 28 Aug 2012; published 2 Nov 2012

4.4. Damage precursor density

The fitting results by the statistical approach (dot line) and the thermal model (solid line) are shown in Fig. 2. The fitted curves by the two methods nearly overlap with an average S value of 3.0×10^{-3} for the statistical approach and 2.7×10^{-3} for the thermal model. Moreover the fitted curves show a good agreement according to the distribution of damage precursor density versus fluence *D(F)*.

The damage precursor densities estimated by both models are presented in Fig. 6 for all the samples. The results by the two methods appear closed. The disagreement in simple SiO_2 sample may be attributed to the lack of data in the large probability region. For each sample the density distribution begins at the damage threshold of the sample, we see a rapid increase at fluences nearby the threshold and this increase slows down with the continuous rise of the fluence. The damage precursor density locates from 0 at the threshold and up to 10^7 /cm^2 at the fluence with 100% damage probability. These orders of magnitude are comparable to the values presented by Laurence et al on fused silica surface at high fluences [8]. Comparing to the mixture of Nb_2O_5, few precursors are found in the mixture of ZrO_2, their curves are closer to the simple SiO_2 curve.

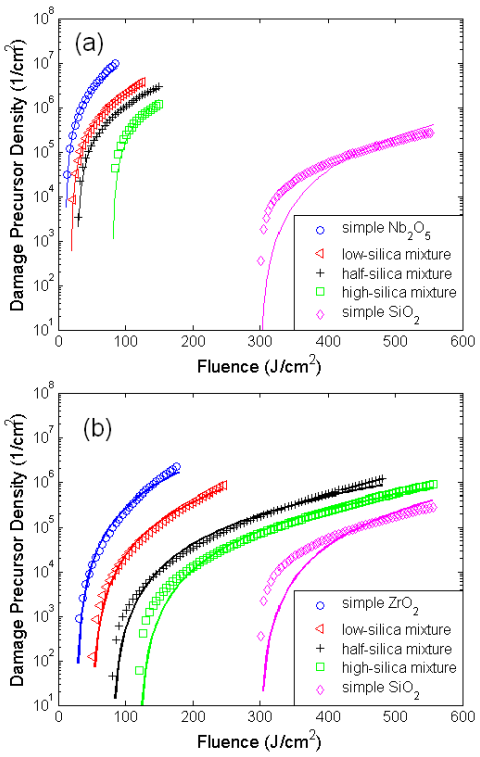

Fig. 6. Distribution versus fluence of damage precursor densities for the two sets of mixtures obtained by the statistical approach (solid line) and the thermal model (symbols): (a) Nb_2O_5/SiO_2 (b) ZrO_2/SiO_2.

4.6 Critical temperature versus band gap

The critical temperatures for each sample are calculated from the LIDT values. The expected order of magnitude is of several thousand degrees, depending on which mechanism is responsible for laser damage. The critical temperatures of the tested samples are summarized versus the band gap in Fig. 7. Band gap dependence is found in those critical temperatures. The simple Nb_2O_5 and its mixtures with band gaps up to 3.94eV (E_{gT}), their critical temperatures remain low and vary from 2000 to 5000 K, while for the set of ZrO_2 samples with band gaps from 4.74 eV to 5.38 eV (E_{gT}), the critical temperatures are between 3800 and 6700 K. The critical temperature of simple SiO_2 with a band gap of 7.54 eV is obtained about 11000 K. It is interesting to compare these values to plasma

#173024 - $15.00 USD Received 20 Jul 2012; revised 24 Aug 2012; accepted 28 Aug 2012; published 2 Nov 2012

temperatures measured by C. W. Carr et al at 1064 nm, 3 ns in several optical materials of different band gaps (see Fig. 7) [22]. The plasma temperature is dependent on the band gap of the material which can be attributed to the large energy needed to liberate an electron in a wider gap material. We observe at 1064 nm that the critical temperatures of simple materials and their mixtures well continue the trend of the plasma temperatures, this could indicate that the critical temperature in the studied mixtures may be related to the plasma temperature.

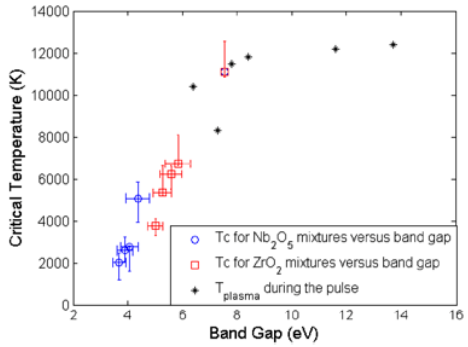

Fig. 7. Critical Temperatures extracted from fitting and Comparison with measured plasma temperatures from Ref [22].

5. Conclusions

Both ZrO_2/SiO_2 and Nb_2O_5/SiO_2 mixtures as well as the simple oxide material coatings were prepared and characterized in terms of damage behavior. The results of the nanosecond LIDT have been reported as a function of the mixture composition and the band gap. The LIDT decreases in both sets of the mixtures with the volumetric fraction of high index material. We find that the nanosecond LIDT of the mixtures is related to the band gap of the material as it has been widely observed in the subpicosecond regime. The damage probability curves have been fitted firstly by a statistical model where the precursor density is proposed to follow a power law versus fluence. Then they were studied by a thermal model based on the photo-induced thermal effect. The thermal model permits to relate the damage probability with the physical properties of mixture and initiating defects. Analysis of RBS has shown an incomplete oxidation of the materials which indicates that metallic or off-stoichiometric oxide defects are candidates as precursors. The influence of these defect types in different mixtures was discussed. We found that only metallic defects with high absorption can explain experimental results. A type of metallic defect with a complex index of 0.3 + 6•i and a maximum radius of 18 nm offered a good interpretation to the performance of damage probability for the whole set of samples. Damage precursor density was estimated by both models, the results show a good agreement between the two models. In addition, a density range up to 10^7 /cm^2 was comparable to the recent reported results for fused silica surface at high fluences. The critical temperatures of both simple materials and mixtures were estimated and thus band gap dependence was obtained. A good agreement was observed with the evolution of plasma temperatures from the literature, this could indicate that the critical temperature in the studied mixtures may be related to the plasma temperature.

Acknowledgments

We acknowledge financial support from Lithuanian Agency for Science, Innovation and Technology grant EIGULYS (Project Nr.31V-140) as well as the Lithuanian French Program Gilibert (the Lithuanian Science Council and the French Foreign Ministry).

#173024 - $15.00 USD Received 20 Jul 2012; revised 24 Aug 2012; accepted 28 Aug 2012; published 2 Nov 2012